RSC Advances

COMMUNICATION

View Article Online
View Journal | View Issue

Cite this: *RSC Adv.*, 2016, **6**, 93343

Received 3rd August 2016
Accepted 25th September 2016

DOI: 10.1039/c6ra19624a

www.rsc.org/advances

Synthesis and NMR analysis of ^{13}C and ^{15}N-labeled long-chain polyamines (LCPAs)†

Maryna Abacilar,[a] Fabian Daus,[a] Christian Haas,[a] Stephan Ingmar Brückner,[b] Eike Brunner*[b] and Armin Geyer*[a]

^{15}N, ^{13}C, or both isotope labels were introduced in selected positions of several LCPAs containing 5, 11, or 13 nitrogens. The number of transformations during chemical synthesis was minimized by coupling Fmoc-glycine-^{15}N, Fmoc-glycine-1-^{13}C, or Fmoc-β-alanine simultaneously at both ends of the growing oligoamide chain on resin-linked norspermidine. LCPAs containing 10–20 nitrogens are the main organic constituent of diatom biosilica. Preliminary NMR studies of bioinspired silica nanocomposites obtained from double-labeled LCPA **14** and ^{29}Si-enriched orthosilicic acid identified the close spatial arrangement of ^{29}Si and ^{13}C nuclei.

Introduction

Long-chain polyamines (LCPAs) have found considerable research interest in the context of silica biomineralisation. These molecules were found to be tightly attached to the biosilica from diatoms[1,2] and sponges.[3] LCPAs could even be detected in sedimented diatom silica from the bottom of the oceans.[4] *In vitro* experiments revealed that LCPAs are capable of accelerating the precipitation of silica from silicic-acid containing solutions.[5] These discoveries have initiated numerous *in vitro* studies as well as biomimetic silica synthesis experiments.[6–11] It is therefore commonly assumed that LCPAs are key molecules for the formation of diatom biosilica. However, the molecular interactions between silicic acid/silica species and LCPAs are not yet fully understood. Solid-state NMR investigations including DNP-enhanced experiments on fully ^{13}C, ^{15}N, and ^{29}Si-labeled diatom biosilica have shown that LCPAs are present at the organic/inorganic interface, *i.e.*, in close contact with the silica.[12,13] Solid-state NMR spectroscopy is in principle able to reveal the interactions at the LCPA–silica interface by using distance-sensitive experiments such as rotational echo double resonance (REDOR[13–16]) and others. This is, however, complicated in fully isotope labeled samples due to signal overlap. Specifically isotope labeled samples are thus highly desirable. The present manuscript describes the synthesis of specifically ^{13}C,^{15}N-labeled LCPAs of similar structure as found in diatoms. It is demonstrated that nanocomposites prepared *in vitro* from these LCPAs and ^{29}Si-labeled silica exhibit remarkable dephasing when rotor-synchronous π pulses are applied at the Larmor frequency of ^{29}Si. That means, the present synthesis and labeling strategies open new perspectives for the application of advanced solid-state NMR techniques to study the interactions between LCPAs and silicic acid/silica species in detail.

Natural LCPAs are microheterogenic mixtures with average chain lengths and variable degrees of methylation. Chemical synthesis allows the incremental variation of LCPA structure and alkylation degree to quantify the markedly different biomineralisation properties of individual LCPA chain lengths.[17] Here, we present recent progress on the synthesis of LCPAs and applications for the site-specific labeling of individual nitrogen and carbon atoms.

Results and discussion

The experimental methodology applied for the synthesis of LCPAs has to take into account the increasing basicity of a growing oligoamine chain. Repeated reductive aminations or *N*-alkylation methods for the assembly of oligoamines containing more than 10 amino groups are hampered by severe analytical problems of the increasingly polar target compounds. Moreover, the analytical purity of synthetic LCPAs is difficult to prove because of non-stoichiometric amounts of TFA and the small ^{1}H NMR chemical shift dispersion of the alkyl groups. In order to avoid polar oligoamine intermediates, we employ a synthetic strategy which evades them before the very last reaction step. For this purpose, we adapted the borane reduction of oligoamides for the synthesis of LCPAs with up to 18

[a]*Fachbereich Chemie, Philipps-University Marburg, Hans-Meerwein-Straße 4, 35032, Marburg, Germany. E-mail: geyer@staff.uni-marburg.de*

[b]*Fachrichtung Chemie und Lebensmittelchemie, TU Dresden, 01062 Dresden, Germany. E-mail: eike.brunner@tu-dresden.de*

† Electronic supplementary information (ESI) available: ^{1}H and ^{13}C NMR, HR-MS and HPLC spectra for all LCPAs and peptide precursors together with ^{1}H NMR and HPLC spectra for the peptides. See DOI: 10.1039/c6ra19624a

nitrogens.[18] The oligoamide precursors are obtained by standard amide coupling methods of solid-phase peptide synthesis and finally reduced on the resin. A test cleavage of the oligoamides from the resin and its analytical proof before the final reduction step is an efficient method to obtain pure LCPAs. The number of chemical transformations is minimized by coupling β-alanine simultaneously on both ends of the growing oligoamide as shown in Fig. 1.

The secondary amino group of norspermidine reacts regioselectively with 2-chlorotrityl chloride resin when its two primary amines are protected with the DDE protecting group [DDE = *N*-(1-(4,4-dimethyl-2,6-dioxocyclohexylidene)ethyl)]. Hydrazinolysis of DDE yields the norspermidine-loaded resin **1a** as shown in Scheme 1 (intermediate oligoamides which are linked to the resin are characterized as "a"). The ^{15}N isotope labels are introduced by coupling of resin **1a** with Fmoc-Gly-^{15}N to obtain **3a**. The test cleavage of a small amount of resin sets free the oligoamide precursor **3b** (test cleavages "b" are characterized in the ESI†). Complete borane reduction of **3a** finally yields the pentaamine LCPA **4** as a TFA salt after acidic cleavage from resin. The isolated LCPA TFA salts are characterized in the Experimental section.

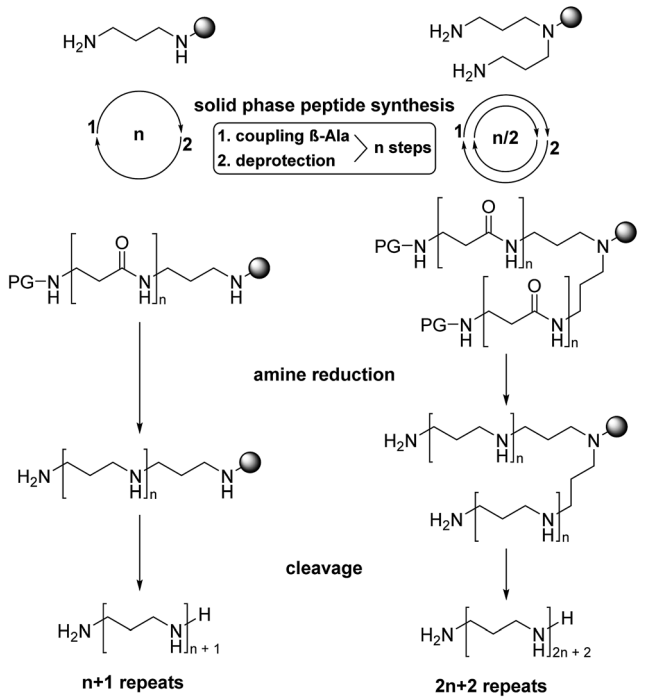

Fig. 1 General synthetic strategy. Propylenediamine or norspermidine were linked to 2-chlorotritylchloride resin (grey shaded circle) and elongated by repeated acylation with Fmoc-β-alanine to the oligoamide precursors of the desired length. Borane reduction followed by TFA cleavage yields the polyamines as TFA salts.

Scheme 2 shows the synthesis of the LCPAs **6**, **8**, and **10** starting either from loaded resin **1a** by automated peptide synthesis on a peptide synthesizer or by manual coupling from **2a**. These three LCPAs have the same number of 13 nitrogens. The isotope label on **10** were introduced in form of ^{13}C-enriched glycine. Scheme 3 shows the synthesis of double-labeled LCPAs **12** and **14** which contain two ^{13}C and two ^{15}N labels each but differ in the position of the label within the LCPA chain.

Fig. 2 shows the ^{13}C and ^{29}Si CP MAS NMR spectra of a dried silica gel prepared from fully ^{29}Si-labeled silicic acid in the presence of compound **14**. The main ^{13}C signal can be assigned to the isotope label as shown in Scheme 3. The assignment of the signals in the ^{29}Si CP MAS NMR spectrum is given in the figure. The result of a ^{1}H–^{13}C–{^{29}Si}–REDOR experiment is shown in Fig. 3 (left).

The REDOR fraction R_f is plotted as a function of echo time $N \times t_r$, *i.e.*, the product of the rotor period t_r and the number of rotor cycles N. The REDOR fraction is defined as $\Delta S/S_0$ with $\Delta S = S - S_0$. S and S_0 are the ^{13}C spin echo amplitudes with and without dephasing pulses for ^{29}Si, respectively. The REDOR fraction increases up to 1 which means that the ^{13}C signal is fully dephased. This remarkably strong REDOR effect indicates a strong ^{13}C–^{29}Si interaction. All ^{13}C labels are obviously in close contact with ^{29}Si in this composite. Analysis of the initial REDOR curve, *i.e.*, for $N \times t_r$ using the approach described by Bertmer and Eckert[19] yields a second moment of 2.0×10^5 Hz^2

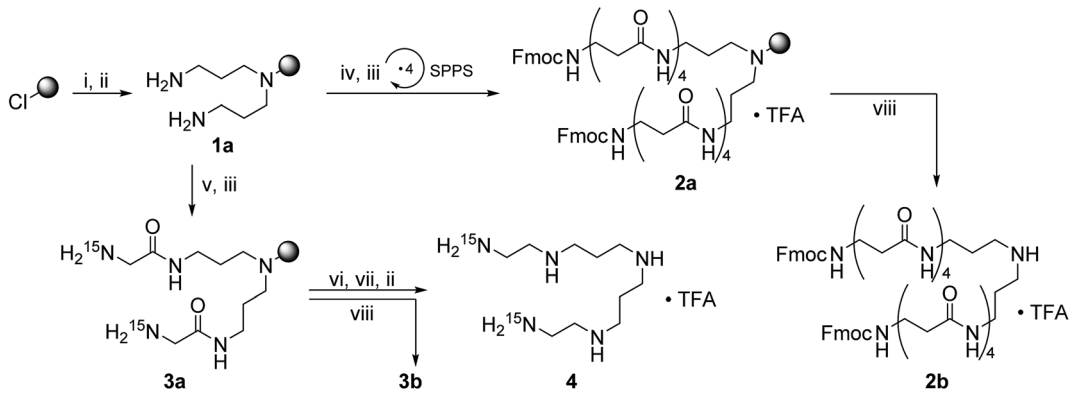

Scheme 1 Synthesis of the ^{15}N-labeld LCPA **4** and resin-linked oligoamide **2a**. A grey shaded circle represents the 2-chlorotritylchloride resin and a downward arrow with the reaction conditions (viii) the NMR test cleavage. (i) 1,9-Bis-DDE-norspermidine, DIPEA, DCM, rt, 16 h; (ii) 2% hydrazine in DMF, rt, 1 h; (iii) 25% piperidine in DMF, rt, 30 min; (iv) Fmoc-β-Ala, HOBt, HBTU, DIPEA, DMF, rt, 1 h; (v) Fmoc-Gly-^{15}N, HOBt, HBTU, DIPEA, DMF, rt, 1 h; (vi) 1.0 M BH_3·THF, 60 °C, 5–7 d; (vii) 25% piperidine in DMF, 60 °C, 2–4 d; (viii) 95% TFA in H_2O.

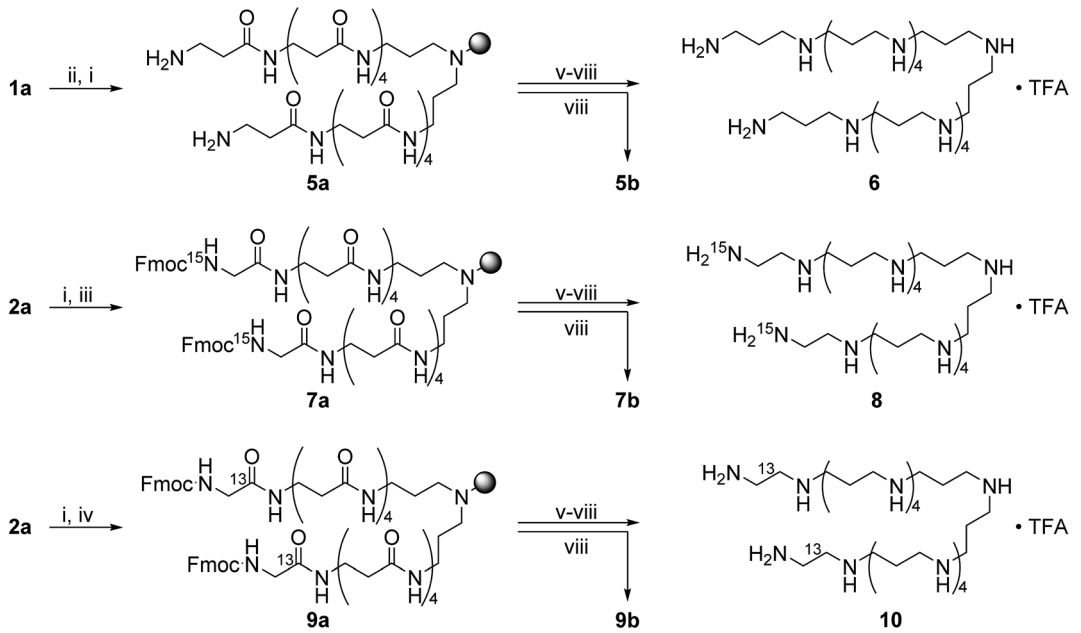

Scheme 2 Synthesis of the LCPAs **6**, **8**, and **10** which are unlabeled or bear a single ^{13}C or ^{15}N label. (i) 25% piperidine in DMF, rt, 30 min; (ii) Fmoc-β-Ala, HOBt, HBTU, DIPEA, DMF, rt, 1 h; (iii) Fmoc-Gly-^{15}N, HOBt, HBTU, DIPEA, DMF, rt, 1 h; (iv) Fmoc-Gly-1-^{13}C, HOBt, HBTU, DIPEA, DMF, rt, 1 h; (v) 1.0 M BH_3·THF, 60 °C, 5–7 d; (vi) 25% piperidine in DMF, 60 °C, 2–4 d; (vii) 2% hydrazine in DMF, rt, 1 h; (viii) 95% TFA in H_2O.

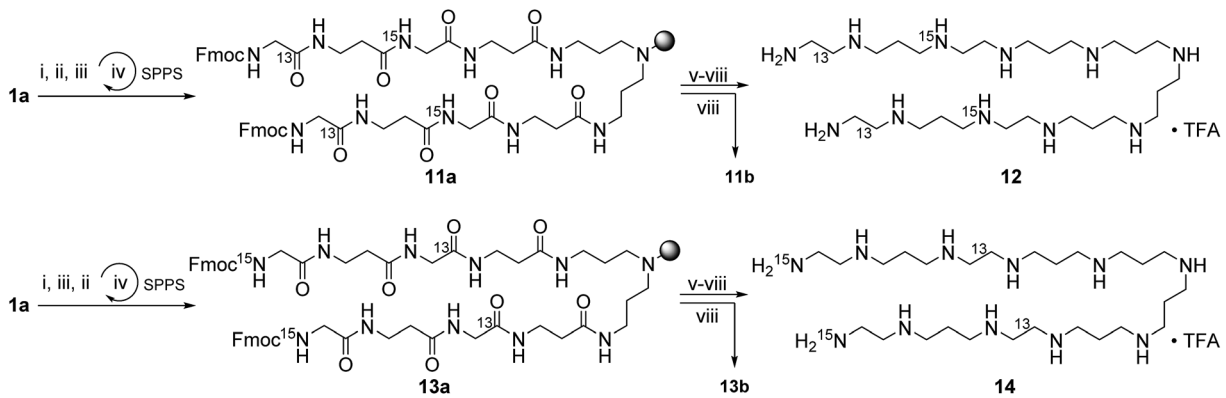

Scheme 3 Synthesis of the double-labeled LCPAs **12**, and **14**. (i) Fmoc-β-Ala, HOBt, HBTU, DIPEA, DMF, rt, 1 h; (ii) Fmoc-Gly-^{15}N, HOBt, HBTU, DIPEA, DMF, rt, 1 h; (iii) Fmoc-Gly-1-^{13}C, HOBt, HBTU, DIPEA, DMF, rt, 1 h; (iv) 25% piperidine in DMF, rt, 30 min; (v) 1.0 M BH_3·THF, 60 °C, 5–7 d; (vi) 25% piperidine in DMF, 60 °C, 2–4 d; (vii) 2% hydrazine in DMF, rt, 1 h; (viii) 95% TFA in H_2O.

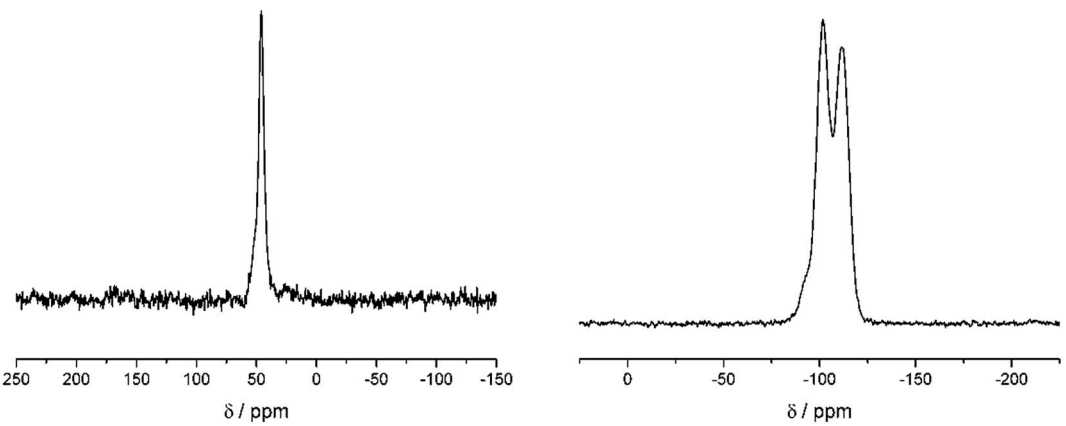

Fig. 2 Left: $^{1}H-^{13}C$ CP Hahn echo spectra of the dried silica gel containing **14** after 2 ms echo time. 2048 scans were acquired. Exponential line broadening set to 50 Hz. Right: $^{1}H-^{29}Si$ CP Hahn echo of the dried silica gel containing **14** after 10 ms echo time indicating the condensation of $Si(OH)_4$ by the appearance of Q^3 and Q^4 groups. 6144 scans were acquired. Exponential line broadening was set to 50 Hz.

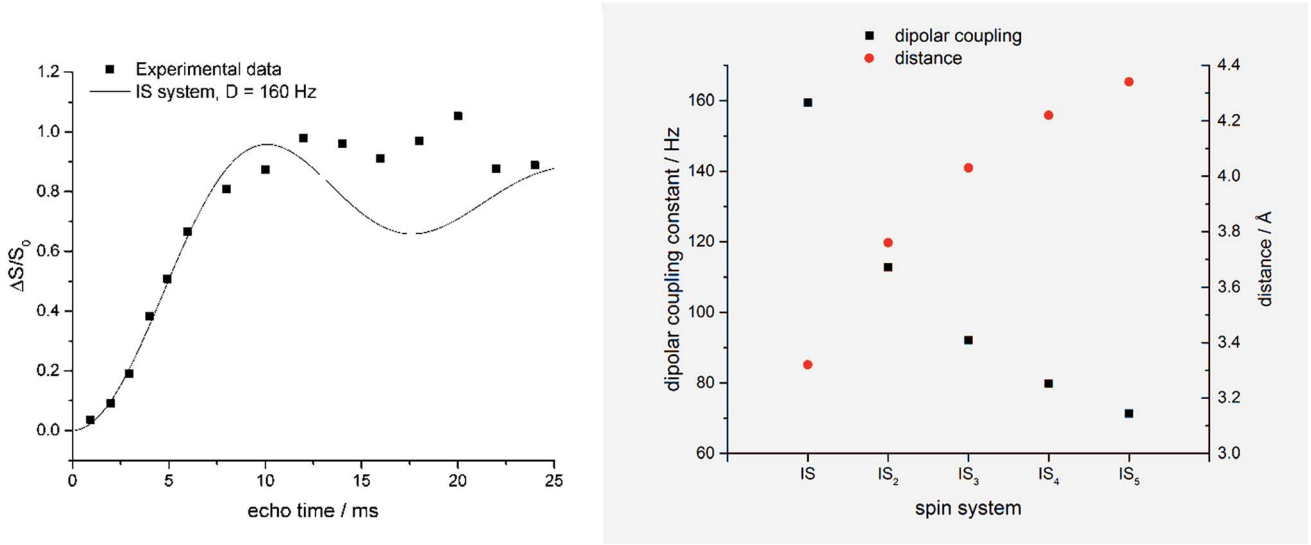

Fig. 3 Left: REDOR fraction ($\Delta S/S_0$) of the dried silica gel containing **14** measured by $^{1}H-^{13}C-\{^{29}Si\}$ CP REDOR. Black line shows simulated curve for a two-spin (IS) system with a dipolar coupling constant of 160 Hz (simulated with Simpson version 4.0.0.[20]). Right: Relation of internuclear distances and individual IS dipolar coupling constants calculated for equidistant IS_n spin systems.

for the $^{13}C-^{29}Si$ dipolar interaction. Using the simple two-spin approximation, this corresponds to a $^{13}C-^{29}Si$ internuclear distance of 3.35 Å. This is unexpectedly low. Furthermore, the two-spin approximation does not describe the measured REDOR curve for long dephasing times. It is, therefore, likely that each carbon label is in contact with more than one ^{29}Si nuclei.

Fig. 3 (right) shows the result of a calculation using the assumption that each ^{13}C nucleus couples with $n = 1$, 2, 3, or 4 equidistant ^{29}Si nuclei. Further experiments and calculations are necessary in order to obtain a more detailed insight into this spin system. In any case, selectively labeled LCPAs form nanocomposites with silicic acid in which they are in very intimate contact with the condensed silica. It is likely that each ^{13}C label is in close proximity of more than one ^{29}Si.

Conclusion

The assembly of LCPAs with 5, 9, to 13 nitrogens bearing site-specific isotope labels (^{13}C, ^{15}N or double-labeled) was achieved by borane reduction of an oligoamide precursor on chlorotrityl resin. The number of chemical transformations was minimized by coupling β-alanine simultaneously at both ends of the growing oligoamide chain on resin-linked norspermidine. Solid state NMR spectroscopy identified the close spatial arrangement of ^{13}C and ^{29}Si nuclei in biomineralized silica obtained from LCPA **14** and orthosilicic acid. The quantitative NMR analysis of LCPAs containing site-specific labels in different positions elucidates molecular details about the relative orientation of LCPAs and the SiO_4 tetrahedron in amorphous silica. Further systematic variations of LCPAs length and labeling position will yield further atomistic details about the borderline between organic and inorganic matter in diatom biosilica and bioinspired silica nanocomposites.

Experimental section

General

All chemicals and solvents used for the synthesis of peptide building blocks or peptide synthesis were purchased from commercial sources and were not purified further. The purification of the peptides was achieved by semipreparative reversed-phase HPLC with a Thermo Scientific Dionex UltiMate 3000 with a MWD-3000 detector and a Macherey-Nagel VP Nucleodur C18 gravity column (5 μm, 125 × 21 mm), using the eluents A: H_2O + 0.1% TFA and B: MeCN + 0.085% TFA. Afterwards, the peptides were lyophilized with a Christ Alpha 2–4 LDplus. The NMR spectroscopy (^{1}H, TOCSY, HSQC, ROESY, ^{13}C) was performed with a Bruker AV-300 or AV-500/HD-500 spectrometer. High-resolution ESI(+) mass spectra were recorded in the positive mode with a Finnigan LTQ-FT from Fisher Thermo Scientific.

Resin loading (1a)

N^1,N^9-Bis-1-(4,4-dimethyl-2,6-dioxo-cyclohexylidene) ethylnorspermidine was prepared from norspermidine (1.0 equiv.) in a reaction with 2-acetyl dimedone (2.0 equiv.) by refluxing in ethanol for 4 h.[21] 2-Chlorotritylchloride resin (1.6 mmol g^{-1}) was loaded with the double-protected norspermidine (6.0–19.0 equiv.) and DIPEA (6.0 equiv.) in DCM (3.0 mL $mmol^{-1}$) at rt for 18 h or 22 h. The resin was filtered, washed with DCM and MeOH (3.0 mL $mmol^{-1}$) two times for 30 min. Finally, the resin was treated several times with a mixture of NEt_3/DMF 1 : 4, DMF, MeOH, DCM before it was dried under vacuum. Then DDE-groups were removed with 2% hydrazine in DMF (vol%) three times for 30 min. The resin was washed several times with DMF, MeOH, DCM before it was dried under vacuum. The loading was determined by NMR test cleavage.

NMR resin test cleavage

A small amount of dry resin (1–2 mg) was treated with trifluoroacetic acid (0.1 mL) at ambient temperature. After 2–5 min DMSO-d_6 (0.5 mL) were added and the ^{1}H NMR was measured of the solution.

Automated solid phase peptide synthesis

Peptide **5a** was synthesized on a microwave equipped CEM Liberty Blue automated peptide synthesizer. The resin **1a** was swollen in DMF for 30 min at ambient temperature. Then resin **1a** was treated with Fmoc-β-Ala (5.0 equiv.), DIC, Oxyma in DMF at 50 °C for 10 min for each active site. Fmoc deprotection was performed with 20% piperidine in DMF for 2.5 min at 50 °C.

Manual solid phase peptide synthesis

Peptide **2a** was synthesized manually. Firstly, the precursor resin **1a** was swollen in DMF for 30 min at ambient temperature under nitrogen atmosphere. Then, the resin was treated with Fmoc-β-Ala (4.0 equiv.), HBTU (4.0 equiv.), HOBt (4.0 equiv.) and DIPEA (4.0 equiv.) in DMF two times for 60 min for each reactive groups. Fmoc deprotection was achieved with 25% piperidine in DMF for 10 min and 20 min followed by the same washing steps.

Coupling of isotope-labeled Fmoc-Gly

The precursor resin **2a** was swollen in DMF for 30 min at ambient temperature under nitrogen atmosphere. The Fmoc group was removed by treatment with 25% piperidine in DMF for 20 min and 10 min followed by the previously mentioned washing steps. Afterwards the resin was treated with Fmoc-Gly-^{15}N (1.5 equiv.), Boc-Gly-^{15}N (1.5 equiv.) or Fmoc-Gly-1-^{13}C (2.0 equiv.), HBTU (2.0 equiv.), HOBt (2.0 equiv.) and DIPEA (4.0 equiv.) in DMF two times for 60 min for each reactive groups. The resin was washed several times with DMF, MeOH and DCM before it was dried under vacuum.

Borane reduction

A solution of borane in THF (1.0 M, 25.0 equiv. per amide) was added to the dry resin under nitrogen atmosphere in a flame-dried flask. After 30 min at ambient temperature, the reaction mixture was heated to 55 °C and kept at this temperature for two to five days depending on the length of the polyamines. Washing with THF and MeOH was followed by alkaline workup. The resin was treated with 25% piperidine in DMF (25.0 mL g^{-1} resin) at 55 °C for two to five days. Finally, the resin was suspended in 2% hydrazine in DMF (10 mL g^{-1} resin). After shaking for 30 min the resin was filtered, washed several times with DMF, MeOH, and DCM, the resin was dried under vacuum.

Cleavage and isolation

The oligoamine was cleaved from the resin with 95% aqueous trifluoroacetic acid. After shaking at ambient temperature for 3 h the resin was filtered and washed with TFA. The combined filtrates were concentrated under reduced pressure and precipitated from cold, dry diethyl ether (30.0 mL). The white solid was washed three times with diethyl ether and lyophilized from water.

LCPA 4

Yield 18.6 mg of yellow foam. ^{1}H NMR (500 MHz, 300 K, DMSO-d_6) δ [ppm] 9.13–8.65 (m, 6H, 1-, 5-NH_2^+, 8-^{15}NH_3^+), 8.12–7.92 (dt, $^1J_{H-^{15}N}$ −73 Hz, 2H, 8-^{15}NH_2), 3.28–3.09 (m, 4H, 7-CH_2), 3.09–2.92 (m, 8H, 4-CH_2, 2-CH_2), 2.67–2.61 (m, 4H, 6-CH_2), 2.01–1.89 (m, 4H, 3-CH_2). ^{13}C NMR (125 MHz, 300 K, DMSO-d_6) δ [ppm] 44.1, 42.6, 32.7, 22.7.

LCPA 6

Yield 26.5 mg of pale yellow foam. ^{1}H NMR (500 MHz, 300 K, DMSO-d_6) δ [ppm] 9.12–8.62 (m, 15H, 1-, 5-, 9-, 13-, 17-, 21-NH_2^+, 25-NH_3^+), 3.27–3.04 (m, 8H, 22-, 24-CH_2), 3.04–2.80 (m, 36H, 4-, 6-, 8-, 10-, 12-, 14-, 16-, 18-, 20-CH_2), 2.14–1.84 (m, 20H, 7-, 11-, 15-, 19-, 23-CH_2), 1.84–1.53 (m, 4H, 2-CH_2), 1.53–1.39 (m, 4H, 3-CH_2). ^{13}C NMR (125 MHz, 300 K, DMSO-d_6) δ [ppm] 52.1, 44.7, 29.6, 23.1, 20.3.

LCPA 8

Yield 65.4 mg of pale yellow foam. ^{1}H NMR (500 MHz, 300 K, DMSO-d_6) δ [ppm] 9.11–8.45 (m, 15H, 1-, 5-, 9-, 13-, 17-, 21-NH_2^+, 24-^{15}NH_3^+), 3.39–3.04 (m, 12H, 4-, 22-, 23-CH_2), 3.04–2.85 (m, 32H, 6-, 8-, 10-, 12-, 14-, 16-, 18-, 20-CH_2), 2.11–1.87 (m, 16H, 7-, 11-, 15-, 19-CH_2), 1.83–1.58 (m, 4H, 2-CH_2), 1.54–1.39 (m, 4H, 3-CH_2). ^{13}C NMR (125 MHz, 300 K, DMSO-d_6) δ [ppm] = 52.6, 50.1, 44.8, 29.6, 23.3, 21.0.

LCPA 10

Yield 17.4 mg of pale yellow foam. ^{1}H NMR (500 MHz, 300 K, DMSO-d_6) δ [ppm] 9.14–8.44 (m, 13H, 1-, 5-, 9-, 13-, 17-, 21-NH_2^+, 24-NH_3^+), 3.30–3.05 (m, 12H, 4-CH_2, 22-^{13}CH_2, 23-CH_2), 3.05–2.80 (m, 32H, 6-, 8-, 10-, 12-, 14-, 16-, 18-, 20-CH_2), 2.15–1.85 (m, 16H, 7-, 11-, 15-, 19-CH_2), 1.76–1.59 (m, 4H, 2-CH_2), 1.51–1.38 (m, 4H, 3-CH_2). ^{13}C NMR (125 MHz, 300 K, DMSO-d_6) δ [ppm] 51.8, 44.2, 42.7, 29.1, 22.5, 19.9.

LCPA 12

Yield 19.7 mg of pale yellow foam. ^{1}H NMR (500 MHz, 300 K, DMSO-d_6) δ [ppm] 9.09–8.52 (m, 13H, 1-, 5-, 9-, 16-NH_2^+, 12-^{15}NH_2^+, 19-NH_3^+), 3.52–3.36 (m, 16H, 10-, 11-, 17-, 18-CH_2), 3.29–3.09 (m, 4H, 4-CH_2), 3.03–2.79 (m, 16H, 6-, 8-, 13-, 15-CH_2), 2.61–2.34 (m, 8H, 7-, 14-CH_2), 2.24–1.89 (m, 4H, 2-CH_2), 1.79–1.59 (m, 4H, 3-CH_2). ^{13}C NMR (125 MHz, 300 K, DMSO-d_6) δ [ppm] 52.2, 42.4, 34.7, 29.5, 22.7, 20.1.

LCPA 14

Yield 28.3 mg of pale yellow foam. ^{1}H NMR (500 MHz, 300 K, DMSO-d_6) δ [ppm] 9.13–8.42 (m, 13H, 1-, 5-, 9-, 12-, 16-NH_2^+, 19-^{15}NH_3^+), 3.53–3.36 (m, 16H, 10-, 11-, 17-, 18-CH_2), 3.34–3.12 (m, 4H, 4-CH_2), 3.02–2.76 (m, 16H, 6-, 8-, 13-, 15-CH_2), 2.58–2.31 (m, 8H, 7-, 14-CH_2), 2.22–1.89 (m, 4H, 2-CH_2), 1.82–1.64 (m, 4H, 3-CH_2). ^{13}C NMR (125 MHz, 300 K, DMSO-d_6) δ [ppm] 52.1, 42.9, 34.8, 29.2, 22.9, 20.5.

Precipitation

Aqueous $^{29}Si(OH)_4$ solution was prepared solving isotopically labeled $Na_2{}^{29}SiO_3$ (synthesized according to ref. 11 and 13) using a vortex mixer and ultrasonic bath in 2100 μL. Meanwhile 5 mg of compound **14** was dissolved in 250 μL ultrapure water. After adding 150 μL 2.4 M HCl to the $^{29}Si(OH)_4$ solution and adjusting its pH value to 7 (only HCl and NaOH were used) the polyamine solution was added. The corresponding tube was then washed with 250 μL water. The washing solution which was also added to the polyamine $^{29}Si(OH)_4$ solution. The pH value was then adjusted to a value of 7.00 ± 0.01 and filled up to 3 ml. The final $^{29}Si(OH)_4$ concentration was 70 μM. The resulting gel was kept at room temperature for 24 h for aging, followed by centrifugation and drying of the centrifugate at 37 °C for 6 days. The dried gel was then filled in solid-state NMR rotors with a diameter of 2.5 mm.

NMR

^1H–^{13}C–{^{29}Si} CP REDOR and the implied ^1H–^{13}C CP HAHN ECHO experiments were acquired employing R_f fields of 120 kHz for ^1H of 60 kHz for ^{13}C and for 55 kHz ^{29}Si for π and π/2 pulses. A ramp of 70–100% was applied to the proton channel while the R_f field of ^{13}C channel kept constant at 60 kHz. The contact time was set to 4 ms and the MAS spinning rate was set to 17 kHz. For proton decoupling SPINAL64 decoupling was applied employing an R_f field of 120 kHz. ^1H–^{29}Si CP HAHN ECHO experiment was acquired employing R_f fields of 120 kHz for ^1H for π/2 pulse of the CP, which also uses a ramp of 70–100%. R_f field strengths of 43.4 kHz and 55 kHz were employed for the ^{29}Si contact pulse for the ^{29}Si π pulses, respectively.

Acknowledgements

This work was supported by the DFG Forschergruppe 2038 "Nanostructured Organic Matrices in Biological Silica Mineralization".

Notes and references

1 N. Kröger, R. Deutzmann, C. Bergsdorf and M. Sumper, *Proc. Natl. Acad. Sci. U. S. A.*, 2000, **97**, 14133.
2 M. Sumper, E. Brunner and G. Lehmann, *FEBS Lett.*, 2005, **579**, 3765.
3 S. Matsunaga, R. Sakai, M. Jimbo and H. Kamiya, *ChemBioChem*, 2007, **8**, 1729.
4 M. C. Bridoux and A. E. Ingalls, *Geochim. Cosmochim. Acta*, 2010, **74**, 4044.
5 T. Mizutani, H. Nagase, N. Fujiwara and H. Ogoshi, *Bull. Chem. Soc. Jpn.*, 1998, **71**, 2017.
6 M. Sumper, S. Lorenz and E. Brunner, *Angew. Chem., Int. Ed.*, 2003, **42**, 5192.
7 E. Brunner, K. Lutz and M. Sumper, *Phys. Chem. Chem. Phys.*, 2004, **6**, 854.
8 P. Behrens, M. Jahns and H. Menzel, The Polyamine Silica System: A Biomimetic Model for the Biomineralization of Silica, in *Handbook of Biomineralization*, ed. E. Bäuerlein, Wiley-VCH, Weinheim, 2007, pp. 2–18.
9 D. J. Belton, S. V. Patwardhan, V. V. Annenkov, E. N. Danilovtseva and C. C. Perry, *Proc. Natl. Acad. Sci. U. S. A.*, 2008, **105**, 5963.
10 V. V. Annenkov, E. N. Danilovtseva, V. A. Pal'shin, V. O. Aseyev, A. K. Petrov, A. S. Kozlov, S. V. Patwardhan and C. C. Perry, *Biomacromolecules*, 2011, **12**, 1772.
11 K. Spinde, K. Pachis, I. Antonakaki, S. Paasch, E. Brunner and K. D. Demadis, *Chem. Mater.*, 2011, **23**, 4676; M. Abacilar, F. Daus and A. Geyer, *Beilstein J. Nanotechnol.*, 2015, **6**, 103; L. Senior, M. P. Crump, C. Williams, P. J. Booth, S. Mann, A. W. Perriman and P. Cumow, *J. Mater. Chem. B*, 2015, **3**, 2607.
12 A. Jantschke, E. Koers, D. Mance, M. Weingarth, E. Brunner and M. Baldus, *Angew. Chem., Int. Ed.*, 2015, **54**, 15069.
13 D. Wisser, S. I. Brückner, F. M. Wisser, G. Althoff-Ospelt, J. Getzschmann, S. Kaskel and E. Brunner, *Solid State Nucl. Magn. Reson.*, 2015, **66**, 33.
14 I. Ben Shir, S. Kababya, T. Amitay-Rosen, Y. S. Balazs and A. J. Schmidt, *J. Phys. Chem. B*, 2010, **114**, 5989.
15 I. Ben Shir, S. Kababya and A. Schmidt, *J. Phys. Chem. C*, 2012, **116**, 9691.
16 T. Gullion and J. Schaefer, *J. Magn. Reson.*, 1989, **81**, 200.
17 A. Bernecker, R. Wieneke, R. Riedel, M. Seibt, A. Geyer and C. Steinem, *J. Am. Chem. Soc.*, 2010, **132**, 1023.
18 D. G. Hall, C. Laplante, S. Manku and J. Nagendran, *J. Org. Chem.*, 1999, **64**, 698; F. Wang, S. Manku and D. G. Hall, *Org. Lett.*, 2000, **2**, 1581; S. Manku, C. Laplante, D. Kopac, T. Chan and D. G. Hall, *J. Org. Chem.*, 2001, **66**, 874.
19 M. Bertmer and H. Eckert, *Solid State Nucl. Magn. Reson.*, 1999, **15**, 139.
20 M. Bak, J. T. Rasmussen and N. C. Nielsen, *J. Magn. Reson.*, 2000, **147**, 296.
21 M. J. Dixon, R. I. Maurer and C. Biggi, *Bioorg. Med. Chem.*, 2005, **13**, 4513.

